



Effects of arm weight support on neuromuscular activation during reaching in chronic stroke patients

Keith D. Runnalls^{1,2} · Pablo Ortega-Auriol^{1,2} · Angus J. C. McMorland^{1,2,3} · Greg Anson^{1,2} · Winston D. Byblow^{1,2} 

Received: 12 June 2019 / Accepted: 7 November 2019 / Published online: 14 November 2019
© Springer-Verlag GmbH Germany, part of Springer Nature 2019

Abstract

To better understand how arm weight support (WS) can be used to alleviate upper limb impairment after stroke, we investigated the effects of WS on muscle activity, muscle synergy expression, and corticomotor excitability (CME) in 13 chronic stroke patients and 6 age-similar healthy controls. For patients, lesion location and corticospinal tract integrity were assessed using magnetic resonance imaging. Upper limb impairment was assessed using the Fugl-Meyer upper extremity assessment with patients categorised as either mild or moderate–severe. Three levels of WS were examined: low = 0, medium = 50 and high = 100% of full support. Surface EMG was recorded from 8 upper limb muscles, and muscle synergies were decomposed using non-negative matrix factorisation from data obtained during reaching movements to an array of 14 targets using the paretic or dominant arm. Interactions between impairment level and WS were found for the number of targets hit, and EMG measures. Overall, greater WS resulted in lower EMG levels, although the degree of modulation between WS levels was less for patients with moderate–severe compared to mild impairment. Healthy controls expressed more synergies than patients with moderate–severe impairment. Healthy controls and patients with mild impairment showed more synergies with high compared to low weight support. Transcranial magnetic stimulation was used to elicit motor-evoked potentials (MEPs) to which stimulus–response curves were fitted as a measure of corticomotor excitability (CME). The effect of WS on CME varied between muscles and across impairment level. These preliminary findings demonstrate that WS has direct and indirect effects on muscle activity, synergies, and CME and warrants further study in order to reduce upper limb impairment after stroke.

Keywords Human · Stroke · Upper limb · Muscle synergy · Reaching · Transcranial magnetic stimulation

Introduction

Stroke is a leading cause of acquired adult disability with two-thirds of stroke survivors experiencing lingering upper limb impairment (Feigin et al. 2010; Mendis 2013). The likelihood of regaining functional independence after stroke is strongly influenced by the initial severity of motor deficits and subsequent recovery of motor function (Kwakkel et al. 1996; Patel et al. 2000; Meijer et al. 2003; Veerbeek et al. 2011). Conventional therapy attempts to engage mechanisms of motor learning to reshape control of the remaining neuro-mechanical repertoire. Task-specific recovery of upper limb function is facilitated when physical therapy exercises are performed with a high number of repetitions (Kwakkel et al. 2004; Veerbeek et al. 2014). However, high repetition schedules are not always achieved (Lang et al. 2009). Providing arm weight support (WS) may augment the performance of arm movements and increase the dose of therapeutic exercise

Communicated by John C. Rothwell.

Electronic supplementary material The online version of this article (<https://doi.org/10.1007/s00221-019-05687-9>) contains supplementary material, which is available to authorized users.

✉ Winston D. Byblow
w.byblow@auckland.ac.nz

- ¹ Movement Neuroscience Laboratory, Department of Exercise Sciences, University of Auckland, Auckland, New Zealand
- ² Centre for Brain Research, University of Auckland, Auckland, New Zealand
- ³ Auckland Bioengineering Institute, University of Auckland, Auckland, New Zealand

that is possible (Kwakkel and Meskers 2014). Studies of WS as an adjuvant to neurorehabilitation have typically included WS as a component of robotic-aided therapies without separating it from other assistive or resistive forces and sensory feedback (Johnson 2006; Loureiro et al. 2011). The separable effects of WS on the upper limb movements of stroke patients has been the subject of less research (Prange et al. 2009a; Krabben et al. 2011); however, progressive shoulder abduction loading appears to be a key component driving improvements in reaching ability with a robotic intervention (Ellis et al. 2018). A better understanding of WS and its underlying neural mechanisms may inform the application of WS in stroke rehabilitation.

In addition to facilitating greater training dosages, WS can also improve movement quality. During reaching tasks, WS reduces antagonist muscle activity in both healthy older adults and chronic stroke patients (Prange et al. 2009a, b). Abnormal coupling of joint torques between the shoulder and elbow is also lessened with WS (Dewald and Beer 2001; Beer et al. 2004). Shoulder abduction loading increases contralesional motor cortical activity and the recruitment of anatomically diffuse reticulospinal motor pathways (McPherson et al. 2018a). The stereotyped flexor synergy can thus be mitigated with WS, permitting greater elbow extension and access to the reaching workspace (Beer et al. 2007; Sukal et al. 2007; Ellis et al. 2017). Taken together, it appears that WS may facilitate a dissociation of strength and motor control deficits. Understanding transient modulation of motor control with WS has relevance because the expressed patterns of neuromotor activity may be reinforced with repetition.

Muscle synergies identified through decomposition of recorded EMG can provide insight into the underlying structure of neuromotor activity. Differences in the recruitment or activation of synergies might reflect context-specific or compensatory motor control, whereas differences in synergy structure might reflect more enduring neuroanatomical constraints. Data obtained from stroke patients performing a dynamic upper limb task confirm that the internal structure of synergies can be preserved despite altered movement performance (Cheung et al. 2009). In contrast, a change in synergy structure was observed in an isometric task where the three heads of the deltoid muscle were consistently expressed as a single synergy and the extent of its activation was related to the degree of impairment (Cheung et al. 2012). Patients with more impairment exhibited fewer synergies, reflecting a lower dimensional neuromechanical repertoire. In healthy adults the level of WS influenced the activation, but not composition, of muscle synergies during a reaching task (Coscia et al. 2014). However, the effect of WS on muscle synergies following stroke, and its interaction with impairment, has not been adequately investigated.

Corticomotor excitability (CME) across the upper limb is modulated with the amount of WS in healthy adults (Runnalls et al. 2014, 2015, 2017). The reduction of antigravity torques required for shoulder abduction has indirect effects on other upper limb muscles through putative neural linkages. To what extent muscle activity and CME are sensitive to partial WS in chronic stroke patients is unknown.

In the present study, we investigated the effects of WS in chronic stroke patients with a range of upper limb impairment. First, we examined upper limb muscle activations during a reaching task. Surface electromyography (EMG) was recorded from eight muscles while participants performed reaching movements to an array of targets with high, medium, and low levels of WS. We expected that greater WS would allow patients to reach more targets. It was hypothesised that support level would interact with impairment severity and target location to modulate integrated EMG area (iEMG) across the upper limb. Second, we conducted a muscle synergy analysis on the EMG data recorded during the reaching task. We hypothesised that patients with more severe impairment would express fewer synergies. We also expected that the application of WS would permit the expression of more synergies. Last, we examined CME at high, medium, and low levels of WS. Transcranial magnetic stimulation (TMS) was used to elicit motor-evoked potentials (MEPs) during a static shoulder abduction task. CME was examined by comparing stimulus–response (SR) curves fitted to means derived from statistical models of MEP area. It was hypothesised that WS would modulate CME, and the pattern of modulation would depend on impairment severity.

Methods

Participants

Thirteen chronic stroke patients (mean age 70.8 years, range 47–88 years, four females) with upper limb impairment participated in this study (Table 1). Patients were included if they reported any degree of upper limb impairment resulting from a first-ever stroke that occurred more than 6 months before testing. Patients were excluded if they had no active range of motion at the shoulder. Patients were excluded from the MRI or TMS component if screening revealed any contraindications. Patients were characterised as having mild impairment if the upper extremity Fugl-Meyer assessment score was 50 or more. Patients with scores below 50 were characterised as moderate–severe (mod–sev). Six neurologically healthy adults (mean age 65.2 years, range 51–71 years, all right dominant, two females) participated as age-similar controls. All participants gave written informed consent. Study procedures were approved by the University

Table 1 Participant characteristics

Participant	Age (years)	Sex	Chronicity (months)	Affected limb	FM	ARAT	MAS	FA _{AI}	Lesion location	Group
1 A	77	M	50	Right	66	57	0	−0.06	Left cerebral white matter	Mild
2 B	80	M	49	Left	45	49	1	0.13	Right cerebral white matter	Mod–Sev
3 C	53	M	40	Right	62	57	0	NA	Left cerebral white matter	Mild
4 D	70	F	90	Right	66	57	0	0.04	Left cerebral cortex	Mild
5 E	74	M	144	Right	12	0	3	0.08	Left cerebral white matter	Mod–Sev
6 F	72	M	104	Right	56	57	1.5	0.05	Left cerebral white matter	Mild
7 G	83	F	43	Right	65	57	0	0.08	Left cerebral cortex	Mild
8 H	72	F	84	Left	9	0	3	0.42	Right cerebral white matter	Mod–Sev
9 I	47	M	39	Right	40	37	2	0.06	Left cerebral white matter	Mod–Sev
10 J	71	F	27	Left	16	3	3	0.17	Right cerebral white matter	Mod–Sev
11 K	88	M	71	Left	58	45	0	0.16	Right cerebral white matter	Mild
12 L	74	M	13	Right	56	53	1	0.15	Left cerebral white matter	Mild
13 M	59	M	167	Left	17	3	1	0.31	Right cerebral white matter	Mod–Sev
Min	47		13		9	0	0	−0.06		
Max	88		167		66	57	3	0.42		
Mean	70.8	9 M 4 F	70.8	8 R 5 L	43.7	36.5	1.2	0.13	2 Cortical 11 subcortical	7 Mild 6 Mod–Sev
14 N	71	M								Control
15 O	69	M								Control
16 P	59	F								Control
17 Q	51	M								Control
18 R	71	M								Control
19 S	70	F								Control
Min	51									
Max	71									
Mean	65.2	4 M 2 F								6 Control

Mild, FM > 50; moderate–severe (Mod–Sev), FM < 50

FM upper extremity Fugl-Meyer score (maximum 66), ARAT action research arm test (maximum 57), MAS modified Ashworth spasticity scale for the elbow (maximum 4), FA_{AI} fractional anisotropy asymmetry index for the posterior limb of the internal capsule (perfect symmetry = 0)

of Auckland Human Participants Ethics Committee in accordance with the Declaration of Helsinki.

Magnetic resonance imaging

Lesion location and corticospinal tract integrity were assessed using magnetic resonance imaging. Brain images were acquired using a 3T MAGNETOM Skyra MRI scanner (Siemens, Germany). An MP-RAGE sequence was used to acquire high-resolution T₁-weighted anatomical images (T_R = 1900 ms, T_E = 2.07 ms, FoV = 256 mm, voxel dimensions of 1.0 × 1.0 × 1.0 mm). Diffusion-weighted images (DWI) were acquired using a single-shot echo-planar imaging sequence (T_R = 3600 ms, T_E = 92.4 ms, FOV = 220 mm, voxel dimensions 2.0 × 2.0 × 2.0 mm), with 30 diffusion gradient orientations (b = 2000 s/mm²).

Lesions were located and masked on T₁-weighted images using FSLView from the FMRIB Software Library

(Jenkinson et al. 2012). Diffusion-weighted images were processed using FMRIB’s Diffusion Toolbox. Images were skull stripped using the Brain Extraction Tool (Smith 2002), and corrected for motion and eddy currents (Jenkinson and Smith 2001; Jenkinson et al. 2002; Andersson and Sotiropoulos 2016). To quantify corticospinal tract (CST) integrity, mean fractional anisotropy (FA) was calculated within the posterior limb of the internal capsule (PLIC) for the ipsilesional (FA_{Ipsi}) and contralesional (FA_{Contra}) hemispheres. A fractional anisotropy asymmetry index (FA_{AI}) was calculated as FA_{AI} = (FA_{Contra} − FA_{Ipsi}) / (FA_{Contra} + FA_{Ipsi}), resulting in a value between −1 and 1 for each participant, where zero indicates perfect symmetry (Stinear et al. 2007). Positive values correspond to reduced ipsilesional FA.

Session order

Participants attended an initial session to complete clinical assessments with a physical therapist. The therapist was not involved in any other aspects of the study. In a subsequent session, participants performed the repeated measures reaching task. Four blocks of reaching trials were completed for high, medium, and low levels of arm weight support. The total 12 blocks were performed in a randomised order. Eligible participants then completed the TMS component in the same session. Single-pulse TMS was used to obtain stimulus–response curves at high, medium, and low levels of arm weight support while participants maintained a static arm posture. Six blocks of stimulation (two for each level of weight support) were performed in a quasi-randomised order. In a separate session, MRI was used to obtain anatomical and diffusion-weighted images (DWI) of the brain. Healthy control participants did not undergo clinical assessments or MRI.

Posture and arm support

The reaching task and TMS measures were completed while participants sat in a chair with their feet on the floor and unsupported arm resting on their lap. Arm weight support was provided to the stroke-affected limb, or dominant limb for healthy controls, by a SaeboMAS arm support system (Saebo Inc., Charlotte, NC). Force was provided by spring tension through a brace that cradled the proximal forearm. The forearm was secured in the brace using elasticised fabric wrap. A standardised static arm position was set with the shoulder elevated approximately 80° (i.e. 10° below the transverse plane) and horizontally flexed 45° forward from the frontal plane, the elbow flexed at 90° , and the forearm pronated palm down. In this position, the hand was in front of the shoulder with the elbow pointing laterally. The brace allowed rotation only around the vertical axis, thus ensuring the forearm was parallel to the floor. Joint angles were initially set using a goniometer and subsequently maintained by aligning the hand to a reference object.

Three levels of arm weight support were defined relative to the force required to compensate for the weight of the arm completely. At the factory-calibrated low support setting (0%), the device carried its weight but provided no additional support to the arm. Individualised levels of support were determined using a force titration procedure. Participants maintained the standardised static arm posture while supportive force was incrementally decreased from a magnitude that required voluntary shoulder adduction. High support (100%) was defined as the last point before root mean square EMG amplitude (rmsEMG) in the anterior deltoid was observed to deflect away from the baseline activity that persists even with excessive support (Runnalls

et al. 2014, 2015, 2017). Medium support was then defined as 50% of high support.

Electromyography

Surface electromyography data were recorded from eight muscles of the supported arm and hand: anterior deltoid (AD), middle deltoid (MD), posterior deltoid (PD), clavicular head of pectoralis major (PM), biceps brachii (BB), lateral head of triceps brachii (TB), brachioradialis (BRD), and extensor carpi radialis (ECR). Self-adhesive Ag–AgCl electrodes (Blue Sensor N; Ambu, Denmark) were placed approximately 2 cm apart in a bipolar montage over the belly of each muscle. The common ground electrode was placed over the acromion process (Red Dot; 3 M Health Care, Canada). Signals were amplified (Grass P511AC; Grass Instrument Division, West Warwick, RI) with $1000\times$ gain, band-pass filtered (10–1000 Hz), sampled at 2 kHz using a 16-bit A/D acquisition system (National Instruments, Austin, TX), and saved for offline analysis.

Reaching task

Participants were seated facing a table-mounted robotic arm (UR5; Universal Robots, Denmark). A push-button assembly was mounted to the tool attachment point of the robot. The 6-cm diameter pushbutton responded to input anywhere on its surface; i.e. finger extension was not required. The robot moved the button to predefined locations to present it as the target for each reach. A trial would begin from a static start position in which the arm was adducted close to the torso with the elbow flexed at 90° and forearm oriented forward orthogonal to the coronal plane. If a participant could not reliably adopt this position, the nearest approximation was used.

Each block of trials was composed of the same sequence of 14 targets (Fig. 1). The targets were located at incrementally greater distances away from the start position along four direction vectors. Targets were grouped in planes 10, 15, 20, and 25 cm anterior to the start position. Low targets were at the same height as the start position. High targets were 10, 20, 30 and 40 cm above the start position. Medial and lateral offsets were symmetrically 5, 10, 15, 20, and 30 cm to the sides of the start position. The distribution was designed to probe the reachable limits of the forward workspace volume. Three targets were located along a low-wide vector, and four targets were located along a high-narrow vector. These vectors were mirrored laterally to test both lateral (ipsilateral) and medial (contralateral) directions.

A computer-generated tone simultaneously started data recording and cued the participant to begin the movement. Participants were instructed to keep their back against the chair and reach to push the button at a comfortable speed.

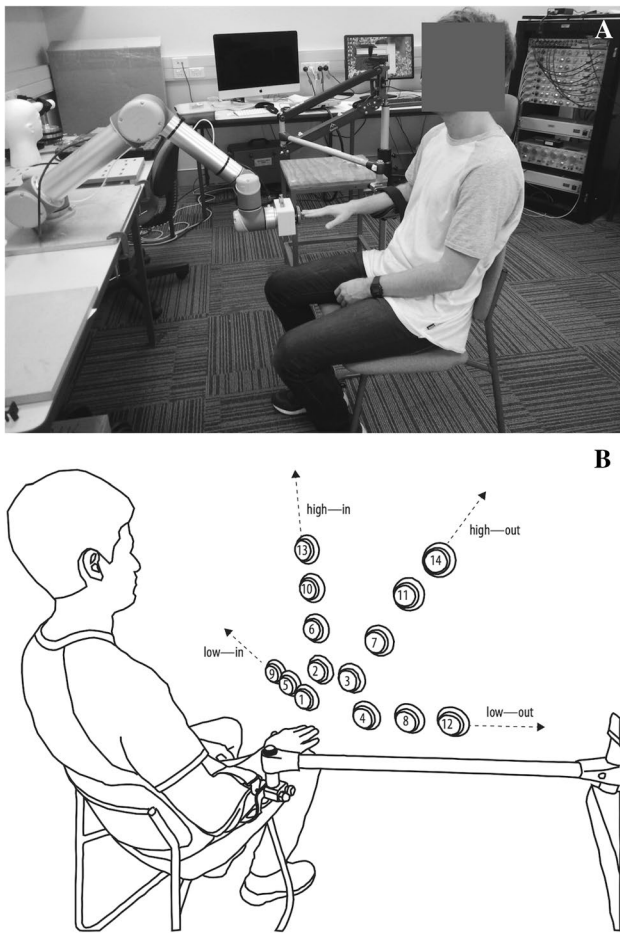


Fig. 1 **a** Demonstration of static start position with the robot presenting the push-button as a calibration point. **b** Schematic illustration of reaching target positions. Targets were presented in numerical order. Targets were 10, 15, 20, and 25 cm anterior to the start position; 0, 10, 20, 30 and 40 cm above the start position; 5, 10, 15, 20, and 30 cm medial/lateral to the start position

Recording terminated when the button was pressed. A trial was flagged as incomplete if the target button could not be pressed without compensatory strategies such as forward torso flexion away from the chair back or stabilisation with the unaffected arm.

Individual EMG traces were detrended, rectified, and low-pass filtered using a fourth-order zero-lag Butterworth filter with a cut-off frequency of 6 Hz using MATLAB R2013a (MathWorks, Natick, MA). The resulting EMG traces from individual muscles were inspected in parallel for each trial and trimmed as necessary to make the EMG onset time consistent between trials. Integrated EMG area (iEMG) was calculated as the dependent measure for each trace.

Statistical analyses

Statistical analyses of the reaching task were conducted using R 3.3.2 (R Core Team 2016) with the *lme4*: Linear Mixed-Effects Models using ‘Eigen’ and S4 (Bates et al. 2015) and *car*: Companion to Applied Regression (Fox and Weisberg 2010) packages. For each participant, iEMG was normalised between zero and one across conditions within each muscle. Linear mixed-effects models were fitted for each muscle to investigate the effects of weight support, impairment severity, and target parameters on muscle activity. In each case, iEMG was modelled as the dependent variable with fixed effects for SUPPORT LEVEL, IMPAIRMENT, TARGET DISTANCE, TARGET HEIGHT, and TARGET SIDE. Random intercepts were included for SUBJECT. Model terms were tested using type II Wald F tests with Kenward–Roger degrees of freedom.

Muscle synergy analysis

Raw EMG traces were detrended, rectified, and normalised to the maximum value across all muscles within each trial. Normalised traces were low-pass filtered using a fourth-order zero-lag Butterworth filter with a cut-off frequency of 6 Hz, then resampled to a length of 1000 points using shape-preserving piecewise cubic interpolation. For each combination of subject and support level, traces were averaged across repetitions to each target and concatenated to an N by T matrix D , where N is the number of EMG channels and T is the number of successfully reached targets multiplied by 1000 (number of data points of EMG trace). D was used as an input to the non-negative matrix factorization algorithm (MATLAB 2016). NMF was modelled as $D = W \times C + \epsilon$, where D is the original data set, W is the synergies, C is the activation coefficient, and ϵ is the approximation error. The algorithm converged onto a constrained solution from 20 consecutive iterations with a difference between iterations of less than 0.01% of the calculated $\|D - W \times C\|$.

The NMF procedure takes as an input parameter the pre-defined number of modules or synergies to extract, between 1 and N . Dimensionality reduction of the original matrix is accomplished by selecting a minimum number of synergies that can reconstruct the matrix D to a certain threshold of quality, quantified by the variance accounted for (VAF). VAF is defined in Eq. 1, where ODS is the variance of the original data set and RD is the variance of the reconstructed data. The number of synergies was determined when $VAF > 90\%$ to reconstruct D , and $VAF > 80\%$ to reconstruct each EMG channel.

$$VAF = 1 - \frac{\sum_{i=1}^n (ODS_i \times RD_i)^2}{\sum_{i=1}^n ODS_i \times \sum_{i=1}^n RD_i^2} \tag{1}$$

A mixed-effects ANOVA ($3_{\text{IMPAIRMENT}} \times 3_{\text{SUPPORT LEVEL}}$) was performed on the number of synergies. Mauchly's test of sphericity was performed and degrees-of-freedom were adjusted using a Greenhouse–Geisser correction ($\epsilon = 0.62$).

Synergy clustering

To compare synergy structures, it is necessary to associate equivalent synergies for each support level and impairment group. Normalised synergies from all participants within a support level and impairment group were pooled for the analysis. Cluster analysis was applied to pooled synergies using K-medoids (Park and Jun 2009) with the scalar product as the distance metric between members and clusters centroids. The number of clusters was fixed to the maximum number of synergies of a participant within the analysed group. Cluster analysis was constrained to avoid the repetition of two or more synergies from a single participant within a cluster. Membership reassignment of synergies was implemented based on the distance metric. The repeated synergy closest to an available cluster without a synergy from that participant was moved. The reassignment process was iterated until no repetitions were found. For each resultant cluster, a mean synergy was calculated. Mean synergies of each impairment group across support level were then pooled together. To match similar synergies across support level, a second cluster analysis was applied to the pooled mean synergies.

Synergy comparison

To determine if synergies were conserved through different support levels, the scalar product was calculated between normalised synergies. The scalar product is a measure of similarity between vectors ranging from 0 (completely different) to 1 (identical). The positivity constraint of NMF means that even two synergies extracted from random data will have non-zero similarity values. Two synergies were defined as similar when their scalar product was above a threshold of the 95th percentile of a z -distribution of scalar products generated by comparing shuffled synergies (Ortega-Auriol et al. 2018). We calculated the distribution of similarity values using synergies constructed from pooled weight values that were randomly shuffled across epochs and muscles.

Transcranial magnetic stimulation

Single-pulse TMS was delivered to M1 using a MagStim 200 magnetic stimulator (Magstim, Dyfed, UK). A figure-of-eight coil (Magstim D70²) was held tangentially to the scalp and angled to direct current in a posterior to anterior

direction across the central sulcus. The coil was positioned at the optimal site for eliciting MEPs in the contralateral BB and ECR muscles and the location was marked on the scalp. Task motor threshold (MT) was defined as the minimum stimulus intensity that elicited a 100 μV MEP in four out of eight trials with the arm in the standardised static position at the high support level. All TMS was conducted while participants performed the static arm abduction task, i.e. actively maintaining the standardised static arm position (illustrated in Runnalls et al. 2014, 2017).

Stimulus–response (SR) curves were collected for high, medium, and low levels of weight support. A single stimulation site was used to concurrently elicit MEPs in all muscles. Five stimulus intensities were set relative to task motor threshold of BB: -5 , $+5$, $+15$, $+25$, and $+35\%$ of maximum stimulator output (% MSO). For each curve, forty stimuli were delivered over two blocks (eight stimuli for each of the five intensities). To mitigate fatigue, participants rested their arm after every four stimuli and proceeded at a self-selected pace.

Raw EMG traces were inspected and processed using Signal 5.11 (CED, Cambridge, UK). Trials were excluded from further analysis if there was no stimulus artefact or if there was phasic muscle activity present. Dependent measures were obtained from individual EMG traces. MEP area was calculated over a 20-ms window determined manually for each muscle. Background muscle activity was calculated as the rmsEMG amplitude over a 50-ms window preceding the stimulus.

Statistical analyses of background muscle activity and MEP area were conducted using R 3.3.2 with the lme4, car, and predictmeans: Calculate Predicted Means for Linear Models packages (Luo et al. 2014). Outliers were identified for each muscle by analysing background muscle activity on a within-participant basis. Observations of rmsEMG more than $1.5 \times$ the interquartile range either above the third quartile or below the first quartile, along with their associated MEP values, were removed from the dataset. MEP area was normalised between zero and one for each participant and muscle, across conditions. Logarithmic transforms were applied to normalised MEP area within the models to better satisfy the assumption of normally distributed residuals.

To assess the effect of WS on background muscle activity, as well as any interaction with impairment severity, linear mixed-effects models were fitted for each muscle. In each case, BACKGROUND MUSCLE ACTIVITY was modelled as the dependent variable with fixed effects for SUPPORT LEVEL and IMPAIRMENT. Random intercepts were included for SUBJECT. Model terms were tested using type II Wald F tests with Kenward–Roger degrees of freedom.

For MEP area, independent linear mixed-effects models were constructed for each muscle. In each case, MEP area was modelled as the dependent variable with fixed effects

for STIMULUS INTENSITY, SUPPORT LEVEL, and IMPAIRMENT. BACKGROUND MUSCLE ACTIVITY (rmsEMG) was included as a continuous covariate term. The error term included random slopes for BACKGROUND MUSCLE ACTIVITY and random intercepts for SUBJECT. The models were then used to predict means and standard errors for MEP area at the median value of the background muscle activity distribution (Welham et al. 2004). This procedure controlled for systematic differences in background muscle activity thus permitting unbiased analysis of MEP area.

Stimulus–response curves were fitted to group level predicted means using nonlinear regression in Prism 7 (GraphPad, San Diego, CA). For each combination of support level and impairment, a three parameter Boltzmann function was fitted to predicted mean MEP area as a function of relative stimulus intensity (Devanne et al. 1997). The upper plateau was constrained to its theoretical range between zero and one to improve the rate at which regression converged on a fit. The slope and half-maximal stimulus intensity (S50) parameters were unconstrained. To test whether changes in support level shifted the stimulus–response curve, extra sum-of-squares F tests were used to assess whether individual regression curves fit the data significantly better than a single curve within each impairment group.

Results

Reaching task

Data from all nineteen participants (six healthy control, seven mild impairment, six moderate–severe impairment) were included in the analysis. The number of targets hit are presented in Fig. 2. Control participants successfully hit all 14 targets at all support levels. Participants with mild upper limb impairment hit an average of 12.8 targets at low support and 12.9 at medium and high support. Those with moderate–severe upper limb impairment hit an average of 8.9 targets at low support, 10.6 at medium, and 11.4 at high. As expected, ANOVA indicated an interaction between IMPAIRMENT and SUPPORT LEVEL ($F_{(4,32)} = 8.63, p = 0.002$).

Means for iEMG are presented in Fig. 3 for each target. Muscles were analysed separately with independent statistical models. Targets were grouped by distance, side, and height to test contrasts. Supplementary Table 1 presents the results of the ANOVA for each muscle.

Effect of weight support on number of synergies

The number of synergies identified for each IMPAIRMENT and SUPPORT LEVEL are presented in Fig. 4. There was no interaction between IMPAIRMENT and SUPPORT LEVEL for the number of synergies, but there were main effects of both factors

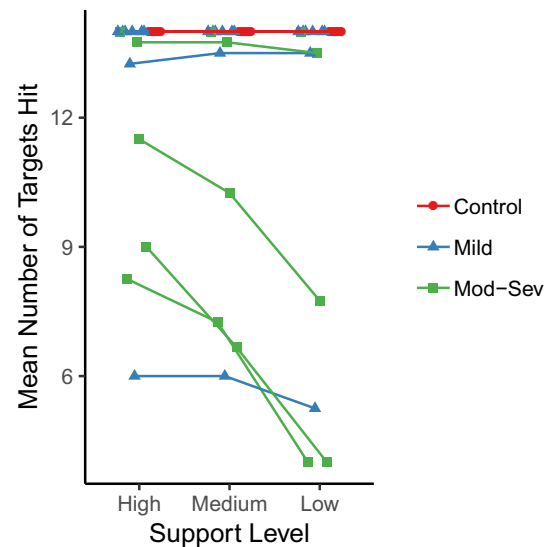


Fig. 2 Mean number of targets hit at each support level for each participant. Colours represent impairment groups. Support level is a discrete variable and data points have been dodged horizontally for visualisation only

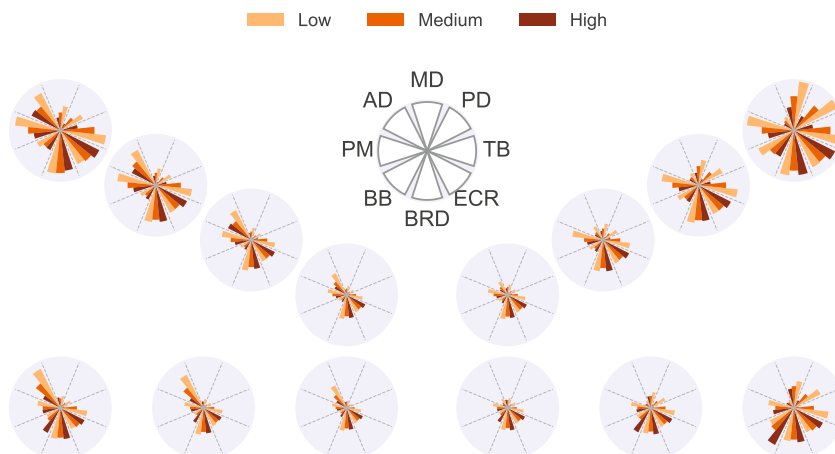
(Table 2). Planned contrasts revealed a greater number of synergies with high support (2.2, SD 1.0) compared to low support (1.6, SD 0.6; $F_{(1,16)} = 7.0, p = 0.018$), with no difference between high and medium support levels (1.8, SD 0.6; $F_{(1,16)} = 1.61, p = 0.22$). The control group expressed more synergies (2.4, SD 0.7) compared to patients with moderate–severe upper limb impairment (1.3, SD 0.8; $d = 1.111, p = 0.02$) while there was no difference between mild (1.86, SD 0.4) and moderate–severe (1.3, SD 0.4; $d = 0.52, p = 0.082$) impairment levels. Given that patients were unable to reach all targets, subsets of the control group data were analysed for comparison to both the four and eight most common targets reached by the patient groups. A one-way repeated measures ANOVA conducted on the four target subset revealed no differences for the number of synergies observed in the control group across SUPPORT LEVEL ($F_{(1.1, 5.4)} = 1.86, p = 0.21, \epsilon = 0.55$).

Functional significance of synergies

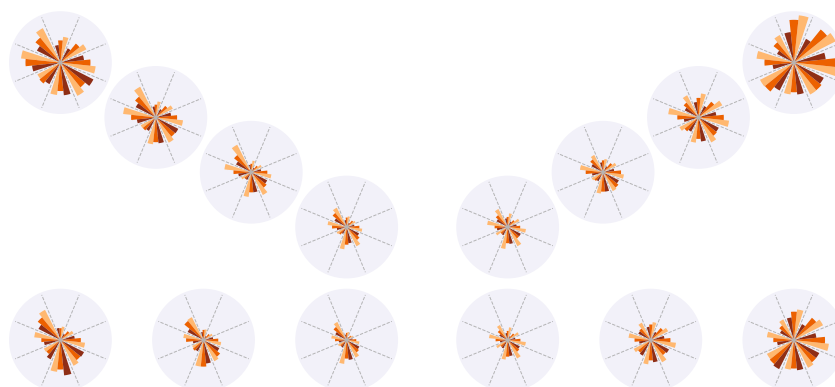
The functional significance of a single synergy is related to the muscle weights in its structure and the reaching targets comprising the data. Four synergies were identified across the different groups and support levels. An internal rotation synergy (S1) was characterised by higher weights of AD and PM. An elbow extension synergy (S2) exhibited a high weight of the TB and a stabilisation role from the deltoid muscles. S2 in the stroke groups showed a high weight on all three deltoid portions, which could reflect a

Fig. 3 Mean normalised iEMG for **a** control, **b** mild, and **c** moderate–severe impairment groups. Each circular subplot corresponds to a reaching target as presented in Fig. 1b. Muscles are represented as sectors of each circle. Support level is indicated by colour

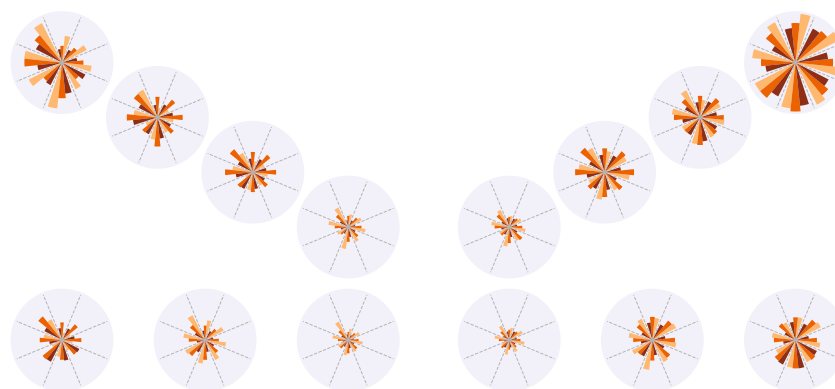
A Control



B Mild



C Mod - Sev



strong atypical deltoid co-contraction. A shoulder flexion synergy (S3) showed higher weights of AD and ECR. A fourth synergy (S4) dominated by ECR and an absence of PM could contribute to the external rotation required for lateral targets. ECR had a high overall contribution across synergies, probably due to the initial pronated arm position.

Synergy similarity

Synergy structures identified by the clustering analysis are presented in Fig. 5. The similarity of synergies was quantified as the average pairwise scalar product within each cluster. The scalar product is a global measure of similarity across synergies. Small differences between synergies in the synergy weight vector space could reflect more considerable

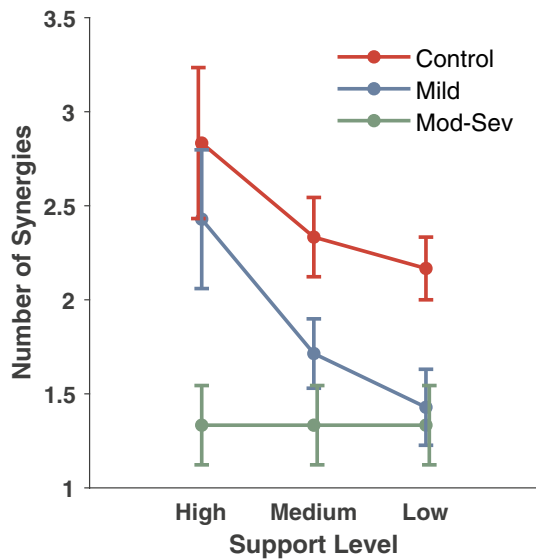


Fig. 4 Mean number of extracted synergies at each support level for each impairment group. Colours represent impairment groups. Error bars indicate ± 1 SEM

Table 2 ANOVA for number of synergies expressed in reaching task

Model term	DF _{num}	DF _{den}	F	p
Support	6.65	1.2	19.9	0.013
Impairment	7.20	2.0	16.0	0.006
Impairment \times support	1.87	2.5	19.9	0.174

differences at the functional level. Thus, despite the similarities that we found across groups, clustered synergies that were different from the control group clusters could be denoted as atypical.

Four synergies were found across all groups and support levels, S1 was present across all groups and support levels with high similarity (0.92, SD 0.05). S2 also showed high similarity (0.87, SD 0.08) and was found across all groups and support levels. S2 showed a lesser degree of co-activation of the deltoids on the control group than in the stroke groups. S3 had a moderate similarity (0.61, SD 0.2) and was present on high and low WS for the control group, and high WS for mild stroke survivors. S4 had a moderate similarity (0.68, SD 0.2) and was recruited during medium WS by the control group and high WS by mild stroke survivors.

Mean pooled similarity across support levels for the mild impairment group was significantly higher than similarity across shuffled synergies (0.6, SD 0.1). A nonparametric ANOVA was used to determine differences between pooled synergy similarity of each group across support levels and the similarity of shuffled synergies. A Kruskal–Wallis test revealed the existence of differences across IMPAIRMENT ($H(3) = 172$), and pairwise comparisons with

Bonferroni-adjusted p values found differences between the control, mild impairment, and moderate–severe impairment groups (all $p < 0.001$) and the shuffled synergies threshold.

Transcranial magnetic stimulation

Data from six control, six mildly impaired, and two moderate–severely impaired participants were included in the analysis. Of the 40 stimuli delivered to each participant per condition, an average of 38.6 traces (range 28–40) were retained in the final analysis. Traces were discarded based on outlying values of background muscle activity. Example EMG traces are presented in Fig. 6.

Effects of weight support and impairment on background muscle activity

Boxplots for background muscle activity are presented in Fig. 7. All muscles exhibited a significant main effect of SUPPORT LEVEL and a significant interaction between SUPPORT LEVEL and IMPAIRMENT (Table 3). With the exception of BB, which exhibited less activity in the control group (0.008 mV) compared to mild (0.026 mV) and moderate–severe (0.021 mV) groups, there were no main effects of IMPAIRMENT.

Effects of weight support and impairment on MEP area and stimulus–response curves

Figure 8 presents stimulus–response data derived from the linear mixed-effects models. Type II Wald χ^2 tests of model terms indicated a significant effect ($p < 0.001$) of SUPPORT LEVEL on MEP area in all muscles. Mean normalised MEP area was then predicted for each combination of STIMULUS INTENSITY, SUPPORT LEVEL, and IMPAIRMENT. The procedure accounted for co-varying background muscle activity. Stimulus–response curves fitted to the predicted means were tested for differences between support levels. Results of the extra sum-of-squares F tests are presented in Table 4.

Discussion

In this study, we examined the interaction between upper limb impairment severity and WS during a reaching task. In support of our hypothesis, there was an interaction between impairment severity and WS on the number of targets hit. As expected, WS had the greatest effect for the moderate–severe impairment group who successfully reached an average of 2.5 more targets with high compared to low WS. An average difference of 0.1 targets for the mild impairment group and 0 targets for the control group is indicative that most participants in these groups could access the entire workspace

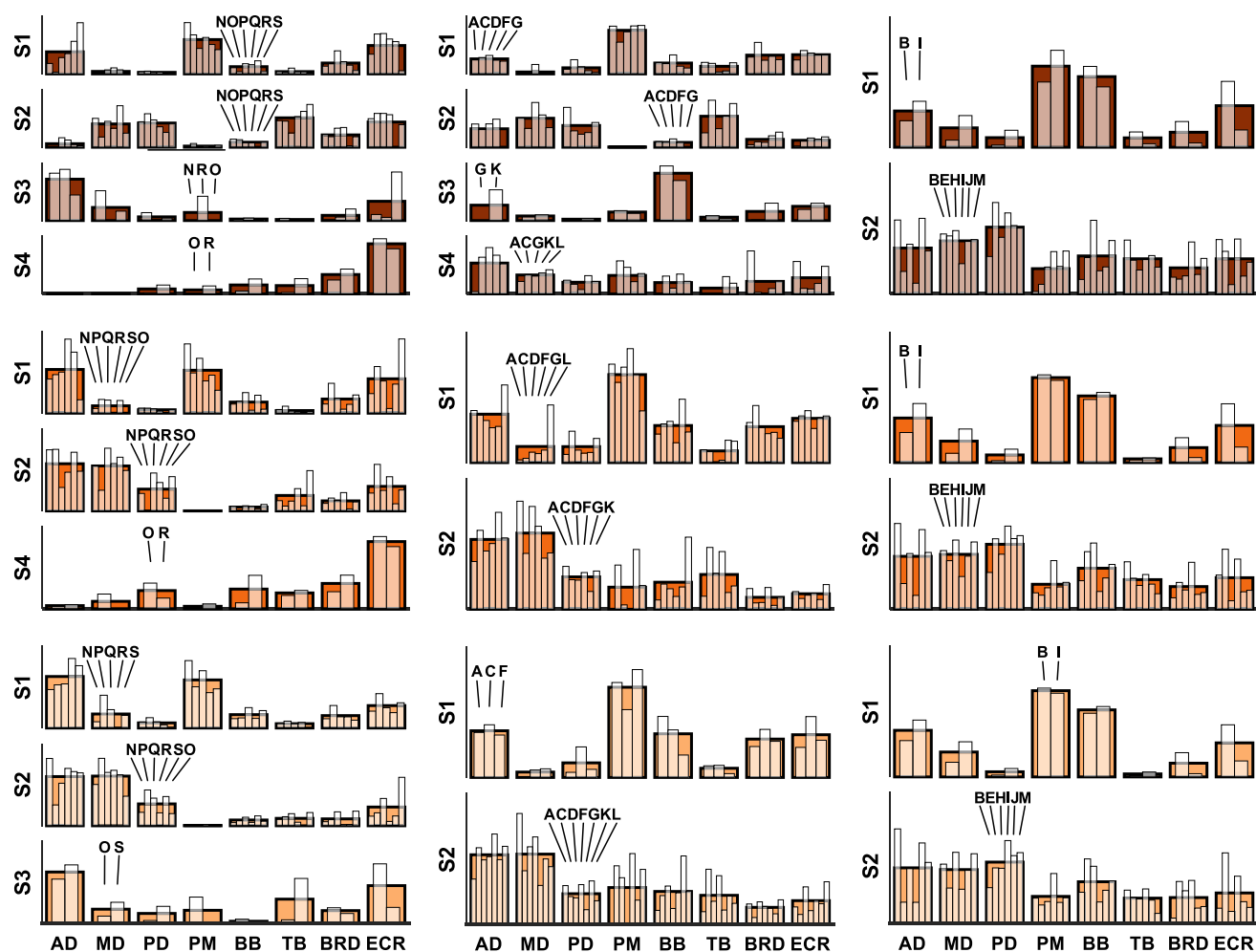


Fig. 5 Composition of individual (white overlaid bars) and mean normalised synergies (coloured bars) for control, mild, and moderate–severe impairment groups (left–right panel columns) across high, medium, and low WS (top–bottom panel rows). Four different synergies (S1–S4) were extracted across groups and conditions. Letters

above white overlaid bars correspond to each participant as presented in Table 1. Muscles are labelled in an abbreviated form (*AD* anterior deltoid, *MD* middle deltoid, *PD* posterior deltoid, *PM* pectoralis major, *BB* biceps brachii, *TB* triceps brachii, *BRD* brachioradialis, *ECR* extensor carpi radialis)

without assistance. In line with previous findings, there was a significant effect of WS on iEMG for all muscles except TB (Prange et al. 2009a, b; Coscia et al. 2014). Those with more severe impairment tended to exhibit smaller magnitudes of iEMG change between support levels. As expected, a muscle synergy analysis revealed that patients with worse impairment exhibited fewer synergies than healthy controls. Individuals in the control and mild impairment groups expressed more synergies with WS, indicating that WS facilitated more complex motor control (Fig. 4). The number of synergies expressed by the moderate–severe impairment group did not respond to changes in WS, likely because of neuroanatomical constraints on available substrates for motor control. In the control group, WS affected CME (MEP area) measured in all muscles except ECR, similar to previous studies with WS and younger participants (Runnalls et al. 2014, 2017).

Although WS influenced CME in both impairment groups, there was not a consistent pattern across muscles (Table 4, Fig. 8). Taken together, these findings provide evidence that WS can influence the upper limb at behavioural and neurophysiological levels across the spectrum of motor impairments resulting from stroke.

Direct and indirect effects of weight support

The direct mechanical action of WS is to reduce the magnitude of anti-gravity torques required at the shoulder. For the AD, MD, PD, and PM muscles, WS significantly lessened both iEMG during reaching (Supplementary Table 1) and rmsEMG during static abduction (Table 3). As expected, high targets required more activity than low targets, and far targets required more activity than near

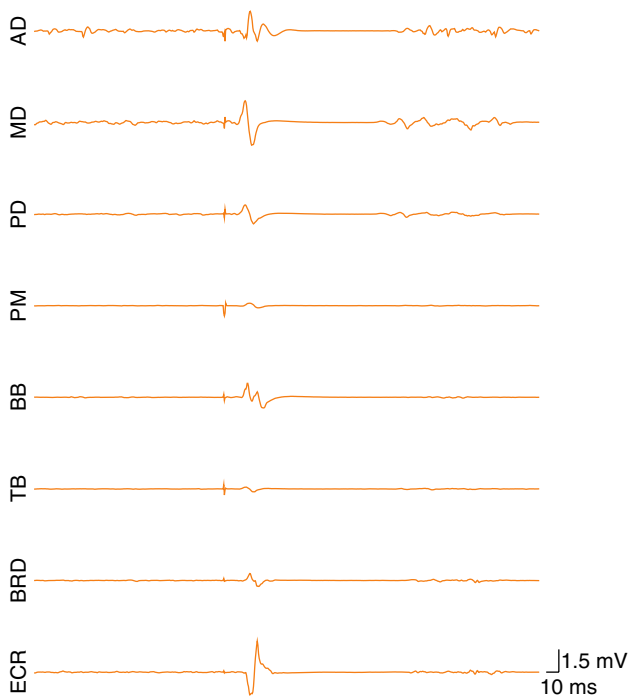


Fig. 6 Single EMG traces showing motor-evoked potentials from a representative participant using the medium support level. TMS intensity was set to task motor threshold + 25% MSO

targets. This pattern was evident across levels of impairment (Fig. 3). Impairment severity interacted with WS during the static abduction task; the moderate–severe group exhibited less modulation of rmsEMG between support levels (Fig. 7). Similarly, the moderate–severe group exhibited less iEMG only with high support. In contrast, the control and mild groups tended to exhibit a more linear response between iEMG and support level similar to previous reports of healthy adults (Coscia et al. 2014). Impairment-dependent responses to WS could result from the recruitment of different neural elements for control. CME was also modulated linearly by WS only in the control and mild groups. Muscle activity patterns for the moderate–severe group are not reflected in the CME data. This disconnect could be a consequence of an increased reliance on alternative motor pathways to drive the proximal upper limb in individuals with significant corticospinal tract damage (Turton et al. 1996; Bradnam et al. 2012; McPherson et al. 2018a). The modulation of muscle activity in AD, MD, PD, and PM is primarily related to the direct mechanical effect of WS on shoulder joint torques. In control and mild groups, the up-regulation of CME with less WS appears to subserve voluntary drive to the proximal upper limb. In the moderate–severe group, neural drive may be distributed through alternative descending

pathways that do not necessarily reflect modulation with WS as change in CME.

Dissociation of elbow muscle activation patterns between dynamic and static tasks provides evidence to support a distinction between direct and indirect effects of WS. A direct mechanical effect of WS is evident for the dynamic reaching task, where the elbow flexors BB and BRD acted against gravity and were sensitive to changes in WS. In contrast, TB was not oriented to act against gravity, thus compensating for gravity with WS was unlikely to have an effect on its activation. This was borne out by the absence of a WS effect on TB activity, which is consistent with previous studies of healthy adults (Prange et al. 2009b; Coscia et al. 2014), and stroke patients (Prange et al. 2009a). Elbow extension for reaching movements may be passively driven by the weight of distal segments, relying on modulation of antagonist elbow flexor tension to permit lengthening. An impaired ability to appropriately modulate BB iEMG for elbow extension may be reflected in the interaction of WS with impairment severity and target height. As expected, high targets required significantly greater BB activity; however, WS affected the groups differently. The application of medium support was sufficient to achieve maximum reduction of BB activity for the control group whereas the moderate–severe group required high support to achieve any change. In both cases, the application of WS through a forearm brace reduced the required force and had the expected effect of directly lessening BB activity.

In contrast to the direct effect of WS on BB activity observed during the reaching task, changes in BB and TB activity with WS during the static arm abduction task reflect an indirect effect of WS (Table 3, Fig. 7). Whereas WS directly impacted the force required for shoulder abduction, BB and TB were oriented to act orthogonal to gravity and were not required to actively perform the task. However, the observed persistence of tonic activity in both muscles and its modulation with WS suggest a distinct mechanism may be responsible. An indirect effect of WS is further supported by changes in CME. The observed modulation of CME with WS in the BB and TB of healthy adults is consistent with previous experiments (Runnalls et al. 2014, 2017). Considering again the task did not require any activity at the elbow, the up-regulation of CME with less WS is likely an indirect effect of altered voluntary drive to proximal muscles mediated through neural linkages. Given that modulation of CME to distal muscles with WS depends on severity of impairment (Table 4), intracortical networks susceptible to disruption by stroke are implicated as a substrate for indirect WS effects. Whether the regulation of CME reflects a functional network architecture or incidental latent connectivity is unknown. In cases of less severe corticospinal system damage, ipsilesional motor cortical areas may provide a substrate well suited for neural reorganisation subserving

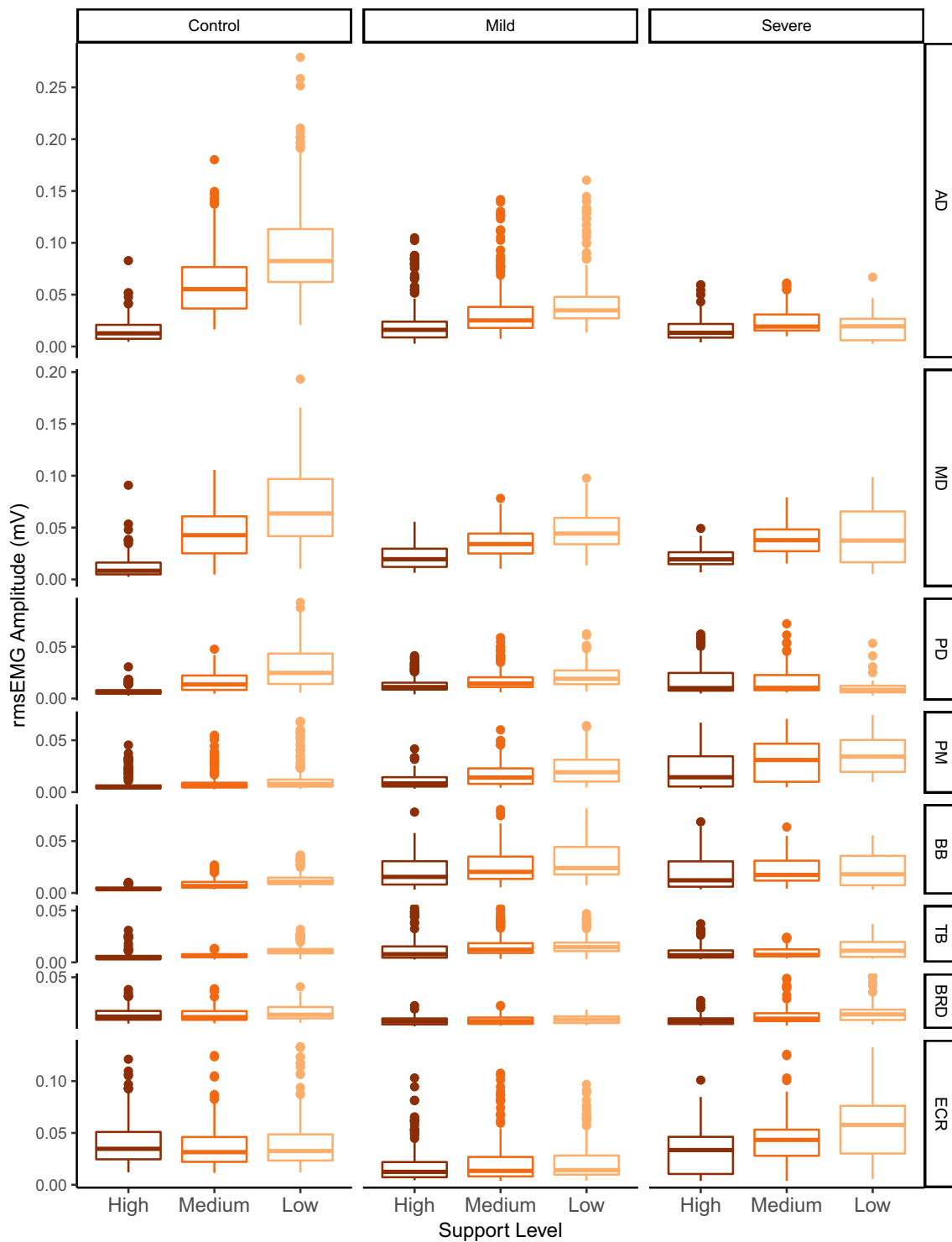


Fig. 7 Background muscle activity at each support level for control, mild, and moderate–severe impairment groups during the standardised static arm abduction task. Boxplots summarise rmsEMG measured before each TMS stimulus

recovery. More severe impairments are associated with the recruitment of remote or secondary motor areas (Cramer et al. 1997; Johansen-Berg et al. 2002; Frost et al. 2003; Fridman et al. 2004). The resulting networks may be less

efficient at generating motor output (Ward et al. 2006; Grefkes and Fink 2011; Yao and Dewald 2018), or involve up-regulation of latent ipsilateral motor pathways with more diverse patterns of innervation (Bradnam et al. 2012;

Table 3 ANOVA for linear mixed models of background muscle activity in static abduction task

Muscle	Model term	DF _{num}	DF _{den}	F	p
AD	Support	2	1620	907.30	<0.001
	Impairment	2	11	2.30	0.147
	Support × impairment	4	1620	149.77	<0.001
MD	Support	2	1624	1140.23	<0.001
	Impairment	2	11	0.12	0.892
	Support × impairment	4	1624	140.31	<0.001
PD	Support	2	1609	376.36	<0.001
	Impairment	2	11	0.69	0.523
	Support × impairment	4	1609	141.06	<0.001
PM	Support	2	1589	370.35	<0.001
	Impairment	2	11	2.41	0.135
	Support × impairment	4	1589	8.54	<0.001
BB	Support	2	1611	368.33	<0.001
	Impairment	2	11	9.71	0.004
	Support × impairment	4	1611	36.16	<0.001
TB	Support	2	1597	242.27	<0.001
	Impairment	2	11	3.09	0.086
	Support × impairment	4	1597	25.20	<0.001
BRD	Support	2	1581	89.47	<0.001
	Impairment	2	11	2.42	0.135
	Support × impairment	4	1581	17.54	<0.001
ECR	Support	2	1588	19.00	<0.001
	Impairment	2	11	2.90	0.097
	Support × impairment	4	1588	18.99	<0.001

McPherson et al. 2018a, b; Karbasforoushan et al. 2019). Mechanism aside, an indirect effect of WS was seen in the modulation of elbow muscle activity during a task in which they were not mechanically involved in gravity compensation and this modulation was smaller with greater severity of impairment.

Variation of muscle activity and CME in distal muscles that are not mechanically involved in gravity compensation provides evidence for an indirect effect of WS. In this study, the orientation and role of ECR was constant for both the reaching and static abduction tasks. However, manipulation of WS altered the amounts of iEMG during reaching and rmsEMG during static abduction (Tables 2 and 3). Similarly, greater iEMG was observed for both high targets and far targets despite requirements for wrist extension not varying between target locations. Modulation of muscle activity in ECR, which was mechanically unrelated to the action of WS, mirrored patterns observed in the proximal upper limb. The present findings suggest WS may influence distal muscle activity indirectly because distal muscles like ECR are subject to common neural drive carried over from proximal muscles. Previous work in both macaques (Zaaimi et al. 2012; Herbert et al. 2015), and humans (Miller and Dewald

2012; Lan et al. 2017), has also reported proximal–distal influences on upper limb muscle activity following stroke.

The interaction of impairment severity and WS for ECR activity and CME was unexpected. During the reaching task, iEMG in the moderate–severe impairment group was lessened only with the highest level of support. Medium support was sufficient to achieve a similar reduction of iEMG for mild impairment. Overall, the patient response may be indicative of a WS threshold phenomenon. The control group paradoxically exhibited the most ECR activity with WS. The cause of this is unclear. It is possible the intact motor system has sufficient physiological range to permit some variation of activity in muscles that do not impact task outcome. A similar argument could explain why ECR CME did not respond to WS in the control and mild groups (Table 4). In contrast, previous experiments with healthy adults found that ECR CME was modulated by WS (Runnalls et al. 2014, 2017). Although it is unknown which factors may account for the discrepancy between studies, the present findings provide evidence in support of an indirect modulation of neural excitability distinct from changes in muscle activity.

Impairment severity and mechanisms for integrated upper limb control

Integrated control of the upper limb based on neural linkages or synergies may facilitate the coordination of voluntary actions like forward reaching. In the present study, indirect effects of WS and interactions with impairment severity provide evidence for integrated control along the proximal–distal axis. Previous reports of distal CME modulation with changes to shoulder activation or shoulder position have interpreted the findings as task-relevant priming for muscle activation (Devanne et al. 2002; Dominici et al. 2005; Ginanneschi et al. 2005, 2006). The present findings support a model in which voluntary drive to proximal muscles acts as a regulatory signal in a proximal–distal hierarchy. Instances of dissociation between CME modulation and muscle activity (cf. Figs. 6 and 7) suggest multiple neural linking mechanisms may be involved (see Runnalls et al. 2015). Along the same lines, different patterns of modulation between muscles could reflect the existence of multiple synergies with complex or competing behaviours. Differential responses depending on impairment severity provide a further indication that integration of control may be accomplished at many levels of the neuraxis.

Indirect responses to upper limb WS after stroke will depend on the neural structures disrupted by the stroke and whether the lesion is up- or downstream of the point where muscle activation information is linked together. Cortical binding of motor commands may be mediated in primary motor cortex where anatomical comingling of muscle representations may facilitate functional interaction (Sanes et al.

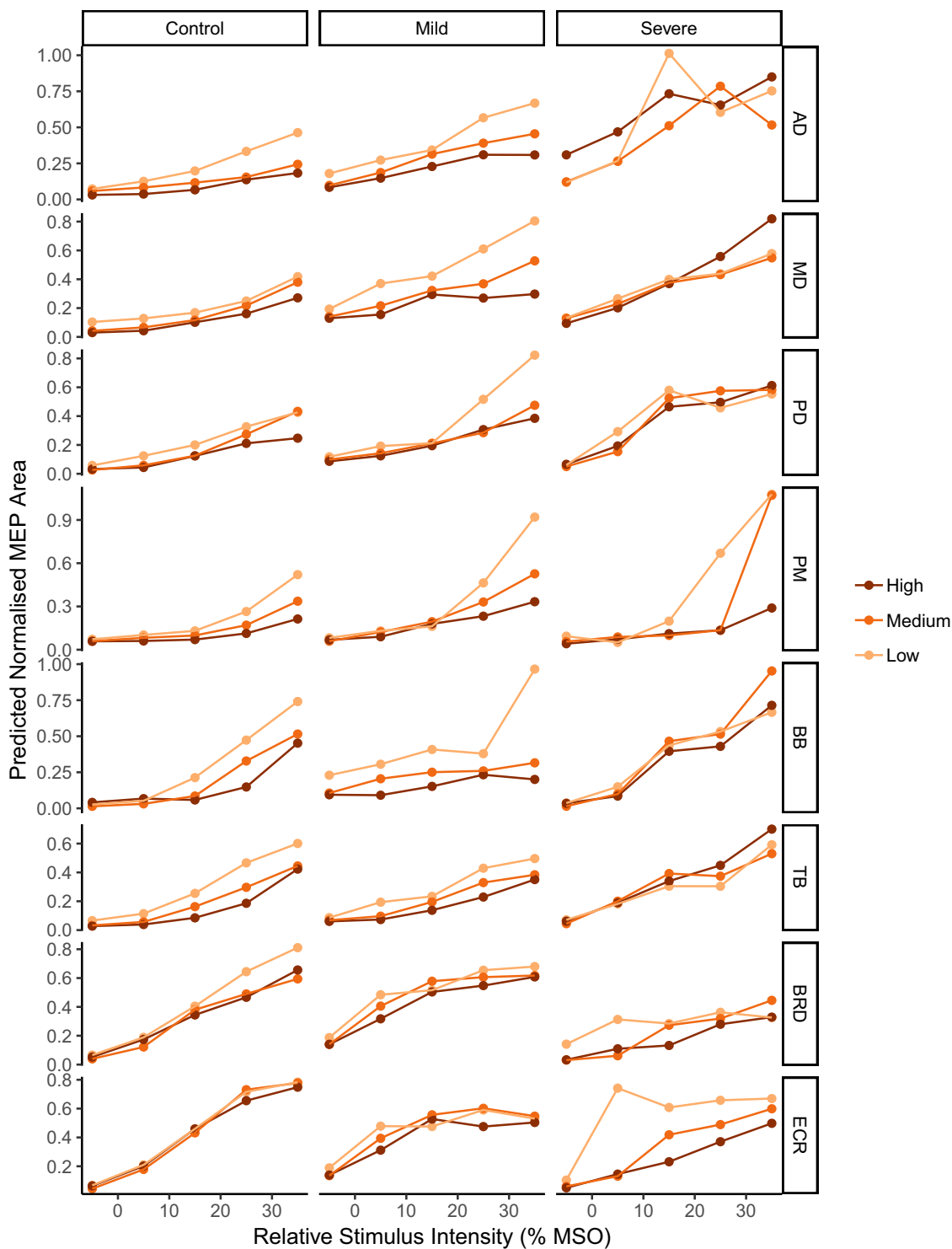


Fig. 8 Predicted mean normalised MEP area is plotted as a function of stimulus intensity at low, medium, and high levels of support for control, mild, and moderate–severe impairment groups. Line shading represents support level

1995; Devanne et al. 2006). Proximal influences on distal CME may involve both intracortical disinhibition (Devanne et al. 2002; Katak et al. 2013) and intracortical facilitation (Ginanneschi et al. 2005, 2006). Subcortical binding

of motor commands may be mediated by divergence of descending corticomotor pathways (McKiernan et al. 1998), recruitment of the cortico-reticulo-proprio-spinal pathway (Pauvert et al. 1998; Pierrot-Deseilligny, 2002), or activation

Table 4 Comparison of stimulus–response curve fits for support levels

Muscle	Impairment group	$F_{(DFn,DFd)}$	p
AD	Control	100.10 _(6, 6)	0.001
	Mild	27.13 _(6, 6)	0.001
	Mod–Sev	0.99 _(6, 6)	0.507
MD	Control	9.16 _(6, 6)	0.008
	Mild	19.88 _(6, 6)	0.001
	Mod–Sev	8.79 _(6, 6)	0.009
PD	Control	61.08 _(6, 6)	<0.001
	Mild	7.68 _(6, 6)	0.013
	Mod–Sev	1.14 _(6, 6)	0.438
PM	Control	8.26 _(6, 6)	0.011
	Mild	13.04 _(6, 6)	0.003
	Mod–Sev	19.62 _(6, 6)	0.001
BB	Control	24.08 _(6, 6)	<0.001
	Mild	3.81 _(6, 6)	0.064
	Mod–Sev	1.01 _(6, 6)	0.494
TB	Control	58.56 _(6, 6)	<0.001
	Mild	8.64 _(6, 6)	0.009
	Mod–Sev	1.14 _(6, 6)	0.439
BRD	Control	9.81 _(6, 6)	0.007
	Mild	2.18 _(6, 6)	0.183
	Mod–Sev	5.68 _(6, 6)	0.026
ECR	Control	1.78 _(6, 6)	0.250
	Mild	1.46 _(6, 6)	0.329
	Mod–Sev	36.66 _(6, 6)	<0.001

Tests where $p < 0.05$ indicate different curves for each support level is the preferred model

of spinal interneuron modules (Bizzi and Cheung 2013). Subcortical lesions at the level of the PLIC would disrupt the pattern of cortically linked neural activity and the activation amplitude of subcortically linked neural activity (McMorland et al. 2015). Any combination of these factors may affect the coordination of descending neural information.

Effects of weight support on muscle synergy expression

Control and mildly impaired participants were able to recruit more complex patterns of muscle activity with WS. The emergence of a higher number of synergies with greater support suggests that WS facilitates independent muscle recruitment. The emergence of new synergies should allow for greater functionality and thus potentially benefit rehabilitation therapy. In contrast, most participants in the moderate–severe impairment group expressed a constant single muscle synergy at all levels of support. Although WS increased the number of targets hit by the moderate–severe

group, it did so without altering the underlying structure of muscle activity.

The number of extracted synergies across groups and WS levels is within the range of 2–8 synergies reported by other studies without constraints over the extracted number of synergies (Flanders and Herrmann 1992; Sabatini 2002; Cheung et al. 2009; Coscia et al. 2014). Several methodological differences can account for the differences in the number of extracted synergies such as VAF percentage threshold, muscles recorded, task spatial exploration, and EMG pre-processing. Nevertheless, the low-pass filter applied to obtain the envelope of the EMG seems to be a significant factor affecting the number of muscle synergies (Kieliba et al. 2018). A lower low-pass filter (6 Hz) will result in a smaller number of extracted synergies compared to studies with a higher low-pass filter (10–20 Hz). The task space constrains the number of synergies and may explain why fewer synergies overall were seen compared with some other studies (Roh et al. 2012). It is possible that with different experimental parameters that allowed more synergies to be identified, we would see the effect of WS in the stroke groups extend also to the low and medium WS levels. Our results agree with the idea of fewer synergies with a lower bandpass and constrained task space.

Interestingly, the number of synergies of the control group appears to increase from three to four synergies by increasing WS level. Several uncertainties exist that may influence the control group result. Arm muscle activation seems to be unchanged by WS in the elderly (Prange et al. 2009a, b), but the effect of WS on synergy structure has not been explicitly studied in this population. In our results all four synergies found with high support were present in the combined medium and low support conditions. While S1 and S2 were common to all conditions, S3 and S4 were extracted from the low and medium WS conditions, respectively. The inconsistent presence of S3 and S4 might be due to the closeness of these synergies to the threshold VAF criteria used to determine a significant number of synergies.

Four synergies were also extracted from the mild impairment group, but only for the high WS condition. Only two synergies were identified with low and medium WS. S3 and S4 in the mild group suggest a function of active elbow flexion and general co-contraction that seem to be atypical given the reaching purpose of the task. The most common S1 and S2 of the mild group reflect a functional internal rotation synergy and an atypical shoulder abduction, respectively. Overall, S2 is the most consistent synergy across all stroke survivor groups, featuring an abnormal co-contraction of the three portions of the deltoid muscles. S2 has been previously described as a significant component of abnormal movement of the upper limb in stroke survivors (Cheung et al. 2009; Roh et al. 2013, 2015). When the WS was increased from low to medium, three extra participants were able to recruit

S1, exemplifying the possibility of more complex and functional patterns with WS.

Most of the participants in the severe group showed a single synergy, except for participants *B* and *I* with two synergies. Participants *B* and *I* had a higher functional level on the clinical scores (FM: $B = 45$, $I = 40$ and ARAT: $B = 49$, $I = 37$) than other moderate–severe participants. The additional synergy S1 of these participants with higher functionality was similar to S1 from the control and mild groups. It is noteworthy that for the moderate–severe group, WS increased the number of targets reached and modulated the magnitude of muscle activity without affecting the number of synergies expressed. This observation demonstrates a dissociation between the amount of muscle activity and the structure of that muscle activity. This could reflect more severe damage to neuroanatomical substrates constraining the neuromechanical repertoire. In this case, increased WS may facilitate positioning of the arm in poses that are otherwise unattainable with the remaining level of neural drive, and which allow improved task performance without improving the muscle activation differentiation possible. In contrast, the control and mild groups expressed more synergies with WS while at a task performance ceiling. This latter observation could indicate that WS can facilitate access to latent regions of the motor control space and improve movement quality by enabling more efficient muscle activity. Whether such phenomena can be meaningfully exploited for neurorehabilitation is an avenue of future research.

Synergy structure overall was conserved across different WS levels including in the presence of neural damage (Israely et al. 2018). Furthermore, synergies in patients with mild impairment were similar to synergies of the control group (Cheung et al. 2009), but exhibiting stereotypical co-activations previously described (Roh et al. 2015). These results, considering the smaller task space, support the idea that more severe damage after stroke leads to a reduced number of synergies (Clark et al. 2010). The number of muscle synergies, therefore, provide a possible marker of neuroanatomical damage (Cheung et al. 2012).

Potential limitations

A limitation of the present study is the absence of kinematic measures of reaching performance. A quantitative characterisation of movement quality could reveal additional effects of WS and add context to the interpretation of EMG data. The reaching task, as defined by the array of targets, was designed to accommodate individuals with a broad range of impairments. However, there was a trade-off in terms of sensitivity to detect changes. Future studies may wish to incorporate more gradations in target location or additional constraints such as a retrieval component. The present study used procedures suitable to obtain only contralateral MEPs

from stimulation of the ipsilesional hemisphere. Additional measures, e.g. ipsilateral MEPs, may have yielded neurophysiological data from more of the patients with severe CST damage. Last, due to individual differences in arm weight and force generating capacity, it is possible that participants were operating at different points within their physiological range of neuromuscular effort at a given level of WS. Expressing or defining WS relative to an individual's maximum effort may provide additional insights into the neurophysiological effects of WS.

Conclusions

Arm weight support may benefit stroke patients with upper limb impairment through both direct and indirect neural mechanisms. First, by directly lessening forces required to complete tasks, individuals with decreased force generating capacity can access a larger workspace and engage in practice with a wider range of tasks. Second, by indirectly influencing linked neural elements, arm weight support may promote a rebalancing of corticomotor excitability in otherwise saturated networks. Potentially, individuals can then engage a neurophysiological landscape more permissive to modulation and plasticity. The threshold of weight support required to achieve a desired modulation will vary between muscles and tasks, and almost certainly depend on the extent of impairment. Keeping these factors in mind, weight support may be a useful adjuvant to upper limb rehabilitation after stroke.

Acknowledgements The authors acknowledge assistance provided by April Ren, Terry Corin, Fiona Doolan, and support from Saebo Inc. for supplying the SaeboMAS. WB received funding from the Health Research Council of New Zealand (Grant No. 14/136).

References

- Andersson JLR, Sotiropoulos SN (2016) An integrated approach to correction for off-resonance effects and subject movement in diffusion MR imaging. *Neuroimage* 125:1063–1078
- Bates D, Mächler M, Bolker BM, Walker SC (2015) Fitting linear mixed-effects models using lme4. *J Stat Softw* 67:1–48
- Beer RF, Dewald JPA, Dawson ML, Rymer WZ (2004) Target-dependent differences between free and constrained arm movements in chronic hemiparesis. *Exp Brain Res* 156:458–470
- Beer RF, Ellis MD, Holubar BG, Dewald JPA (2007) Impact of gravity loading on post-stroke reaching and its relationship to weakness. *Muscle Nerve* 36:242–250
- Bizzi E, Cheung VCK (2013) The neural origin of muscle synergies. *Front Comput Neurosci* 7:1–6
- Bradnam LV, Stinear CM, Barber PA, Byblow WD (2012) Contralateral hemisphere control of the proximal paretic upper limb following stroke. *Cereb Cortex* 22:2662–2671

- Cheung VCK, Piron L, Agostini M, Silvoni S, Turolla A, Bizzi E (2009) Stability of muscle synergies for voluntary actions after cortical stroke in humans. *Proc Natl Acad Sci USA* 106:19563–19568
- Cheung VCK, Turolla A, Agostini M, Silvoni S, Bennis C, Kasi P, Paganoni S, Bonato P, Bizzi E (2012) Muscle synergy patterns as physiological markers of motor cortical damage. *Proc Natl Acad Sci USA* 109:14652–14656
- Clark DJ, Ting LH, Zajac FE, Neptune RR, Kautz SA (2010) Merging of healthy motor modules predicts reduced locomotor performance and muscle coordination complexity post-stroke. *J Neurophysiol* 103:844–857
- Coscia M, Cheung VCK, Tropea P, Koenig A, Monaco V, Bennis C, Micera S, Bonato P (2014) The effect of arm weight support on upper limb muscle synergies during reaching movements. *J NeuroEng Rehabil* 11:1–15
- Cramer SC, Nelles G, Benson RR, Kaplan JD, Parker RA, Kwong KK, Kennedy DN, Finklestein SP, Rosen BR (1997) A functional MRI study of subjects recovered from hemiparetic stroke. *Stroke* 28:2518–2527
- Devanne H, Lavoie BA, Capaday C (1997) Input-output properties and gain changes in the human corticospinal pathway. *Exp Brain Res* 114:329–338
- Devanne H, Cohen LG, Kouchtir-Devanne N, Capaday C (2002) Integrated motor cortical control of task-related muscles during pointing in humans. *J Neurophysiol* 87:3006–3017
- Devanne H, Cassim F, Ethier C, Brizzi L, Thevenon A, Capaday C (2006) The comparable size and overlapping nature of upper limb distal and proximal muscle representations in the human motor cortex. *Eur J Neurosci* 23:2467–2476
- Dewald JPA, Beer RF (2001) Abnormal joint torque patterns in the paretic upper limb of subjects with hemiparesis. *Muscle Nerve* 24:273–283
- Dominici F, Popa T, Ginanneschi F, Mazzocchio R, Rossi A (2005) Cortico-motoneuronal output to intrinsic hand muscles is differentially influenced by static changes in shoulder positions. *Exp Brain Res* 164:500–504
- Ellis MD, Schut I, Dewald JPA (2017) Flexion synergy overshadows flexor spasticity during reaching in chronic moderate to severe hemiparetic stroke. *Clin Neurophysiol* 128(7):1308–1314
- Ellis MD, Carmona C, Drogos J, Dewald JPA (2018) Progressive abduction loading therapy with horizontal-plane viscous resistance targeting weakness and flexion synergy to treat upper limb function in chronic hemiparetic stroke: a randomized clinical trial. *Front Neurol* 9:71
- Feigin VL, Barker-Collo S, Parag V, Senior H, Lawes CMM, Ratnasabapathy Y, Glen E, ASTRO study group (2010) Auckland Stroke Outcomes Study. Part 1: gender, stroke types, ethnicity, and functional outcomes 5 years poststroke. *Neurology* 75:1597–1607
- Flanders M, Herrmann U (1992) Two components of muscle activation: scaling with the speed of arm movement. *J Neurophysiol* 67:931–943
- Fox J, Weisberg S (2010) *An R companion to applied regression*, 2nd edn. SAGE, Thousand Oaks
- Fridman EA, Hanakawa T, Chung M, Hummel F, Leiguarda RC, Cohen LG (2004) Reorganization of the human ipsilesional premotor cortex after stroke. *Brain* 127:747–758
- Frost SB, Barbay S, Friel KM, Plautz EJ, Nudo RJ (2003) Reorganization of remote cortical regions after ischemic brain injury: a potential substrate for stroke recovery. *J Neurophysiol* 89:3205–3214
- Ginanneschi F, Santo F, Dominici F, Gelli F, Mazzocchio R, Rossi A (2005) Changes in corticomotor excitability of hand muscles in relation to static shoulder positions. *Exp Brain Res* 161:374–382
- Ginanneschi F, Dominici F, Biasella A, Gelli F, Rossi A (2006) Changes in corticomotor excitability of forearm muscles in relation to static shoulder positions. *Brain Res* 1073–1074:332–338
- Grefkes C, Fink GR (2011) Reorganization of cerebral networks after stroke: new insights from neuroimaging with connectivity approaches. *Brain* 134:1264–1276
- Herbert WJ, Powell K, Buford JA (2015) Evidence for a role of the reticulospinal system in recovery of skilled reaching after cortical stroke: initial results from a model of ischemic cortical injury. *Exp Brain Res* 233(11):3231–3251
- Israely S, Leisman G, Machluf CC, Carmeli E (2018) Muscle synergies control during hand-reaching tasks in multiple directions post-stroke. *Front Comput Neurosci* 12:10
- Jenkinson M, Smith S (2001) A global optimisation method for robust affine registration of brain images. *Med Image Anal* 5:143–156
- Jenkinson M, Bannister P, Brady M, Smith S (2002) Improved optimization for the robust and accurate linear registration and motion correction of brain images. *Neuroimage* 17:825–841
- Jenkinson M, Beckmann CF, Behrens TEJ, Woolrich MW, Smith SM (2012) FSL. *Neuroimage* 62:782–790
- Johansen-Berg H, Rushworth MFS, Bogdanovic MD, Kischka U, Wimalaratna S, Matthews PM (2002) The role of ipsilateral premotor cortex in hand movement after stroke. *Proc Natl Acad Sci USA* 99:14518–14523
- Johnson MJ (2006) Recent trends in robot-assisted therapy environments to improve real-life functional performance after stroke. *J NeuroEng Rehabil* 3:29
- Kantak SS, Wittenberg GF, Liao W-W, Magder LS, Rogers MW, Waller SM (2013) Posture-related modulations in motor cortical excitability of the proximal and distal arm muscles. *Neurosci Lett* 533:65–70
- Karbasforoushan H, Cohen-Adad J, Dewald JPA (2019) Brainstem and spinal cord MRI identifies altered sensorimotor pathways post-stroke. *Nat Commun* 10(1):3524
- Kieliba P, Tropea P, Pirondini E, Coscia M, Micera S, Artoni F (2018) How are muscle synergies affected by electromyography pre-processing? *IEEE Trans Neural Syst Rehabil Eng* 26:882–893
- Krabben T, Prange GB, Molier BI, Stienen AHA, Jannink MJA, Buurke JH, Rietman JS (2011) Influence of gravity compensation training on synergistic movement patterns of the upper extremity after stroke, a pilot study. *J NeuroEng Rehabil* 9:44
- Kwakkel G, Meskers CGM (2014) Effects of robotic therapy of the arm after stroke. *Lancet Neurol* 13:132–133
- Kwakkel G, Wagenaar RC, Kollen BJ, Lankhorst GJ (1996) Predicting disability in stroke—a critical review of the literature. *Age Ageing* 25:479–489
- Kwakkel G, van Peppen R, Wagenaar RC, Wood Dauphinee S, Richards C, Ashburn A, Miller K, Lincoln N, Partridge C, Wellwood I, Langhorne P (2004) Effects of augmented exercise therapy time after stroke: a meta-analysis. *Stroke* 35:2529–2539
- Lan Y, Yao J, Dewald JPA (2017) The impact of shoulder abduction loading on volitional hand opening and grasping in chronic hemiparetic stroke. *NRR* 31(6):521–529
- Lang CE, Macdonald JR, Reisman DS, Boyd L, Jacobson Kimberley T, Schindler-Ivens SM, Hornby TG, Ross SA, Scheets PL (2009) Observation of amounts of movement practice provided during stroke rehabilitation. *Arch Phys Med Rehabil* 90:1692–1698
- Loureiro RCV, Harwin WS, Nagai K, Johnson M (2011) Advances in upper limb stroke rehabilitation: a technology push. *Med Biol Eng Comput* 49:1103–1118
- Luo D, Ganesh S, Koolgaard J (2014) Predictmeans: calculate predicted means for linear models. <http://cran.r-project.org/web/packages/predictmeans/index.html>. Accessed 1 Dec 2016
- MATLAB (2016). Version 9.1 (R2016b) In: The Mathworks Inc, Natick, Massachusetts
- McKiernan BJ, Marcario JK, Karrer JH, Cheney PD (1998) Cortico-motoneuronal postspike effects in shoulder, elbow, wrist, digit, and intrinsic hand muscles during a reach and prehension task. *J Neurophysiol* 80:1961–1980

- McMorland AJC, Runnalls KD, Byblow WD (2015) A neuroanatomical framework for upper limb synergies after stroke. *Front Hum Neurosci* 9:305
- McPherson JG, Chen A, Ellis MD, Yao J, Heckman CJ, Dewald JPA (2018a) Progressive recruitment of contralesional cortico-reticulospinal pathways drives motor impairment post stroke. *J Physiol* 596(7):1211–1225
- McPherson JG, Ellis MD, Harden RN, Carmona C, Heckman CJ, Dewald JPA (2018b) Neuromodulatory inputs to motoneurons contribute to the loss of independent joint control in chronic moderate to severe hemiparetic stroke. *Front Neurol* 9:470
- Meijer R, Ihnenfeldt DS, de Groot IJM, van Limbeek J, Vermeulen M, de Haan RJ (2003) Prognostic factors for ambulation and activities of daily living in the subacute phase after stroke. A systematic review of the literature. *Clin Rehabil* 17:119–129
- Mendis S (2013) Stroke disability and rehabilitation of stroke: world Health Organization perspective. *Int J Stroke* 8:3–4
- Miller LC, Dewald JPA (2012) Involuntary paretic wrist/finger flexion forces and EMG increase with shoulder abduction load in individuals with chronic stroke. *Clin Neurophysiol* 123(6):1216–1225
- Ortega-Auriol PA, Besier TF, Byblow WD, McMorland AJC (2018) Fatigue influences the recruitment, but not structure, of muscle synergies. *Front Hum Neurosci* 12:217. <https://doi.org/10.3389/fnhum.2018.00217>
- Park H-S, Jun C-H (2009) A simple and fast algorithm for K-medoids clustering. *Expert Syst Appl* 36:3336–3341
- Patel AT, Duncan PW, Lai SM, Studenski S (2000) The relation between impairments and functional outcomes poststroke. *Arch Phys Med Rehabil* 81:1357–1363
- Pauvert V, Pierrot-Deseilligny E, Rothwell JC (1998) Role of spinal premotoneurons in mediating corticospinal input to forearm motoneurons in man. *J Physiol (Lond)* 508(Pt 1):301–312
- Pierrot-Deseilligny E (2002) Propriospinal transmission of part of the corticospinal excitation in humans. *Muscle Nerve* 26:155–172
- Prange GB, Jannink MJA, Stienen AHA, van der Kooij H, IJzerman MJ, Hermens HJ (2009a) Influence of gravity compensation on muscle activation patterns during different temporal phases of arm movements of stroke patients. *NRR* 23:478–485
- Prange GB, Kallenberg LAC, Jannink MJA, Stienen AHA, van der Kooij H, IJzerman MJ, Hermens HJ (2009b) Influence of gravity compensation on muscle activity during reach and retrieval in healthy elderly. *J Electromyogr Kinesiol* 19:e40–e49
- Roh J, Rymer WZ, Beer RF (2012) Robustness of muscle synergies underlying three-dimensional force generation at the hand in healthy humans. *J Neurophysiol* 107:2123–2142
- Roh J, Rymer WZ, Perreault EJ, Yoo SB, Beer RF (2013) Alterations in upper limb muscle synergy structure in chronic stroke survivors. *J Neurophysiol* 109:768–781
- Roh J, Rymer WZ, Beer RF (2015) Evidence for altered upper extremity muscle synergies in chronic stroke survivors with mild and moderate impairment. *Front Hum Neurosci* 9:6
- Runnalls KD, Anson G, Wolf SL, Byblow WD (2014) Partial weight support differentially affects corticomotor excitability across muscles of the upper limb. *Physiol Rep* 2:e12183
- Runnalls KD, Anson G, Byblow WD (2015) Partial weight support of the arm affects corticomotor selectivity of biceps brachii. *J NeuroEng Rehabil* 12:1–10
- Runnalls KD, Anson G, Byblow WD (2017) Posture interacts with arm weight support to modulate corticomotor excitability to the upper limb. *Exp Brain Res* 235:97–107
- Sabatini AM (2002) Identification of neuromuscular synergies in natural upper-arm movements. *Biol Cybern* 86:253–262
- Sanes JN, Donoghue JP, Thangaraj V, Edelman RR, Warach S (1995) Shared neural substrates controlling hand movements in human motor cortex. *Science* 268:1775–1777
- Smith SM (2002) Fast robust automated brain extraction. *Hum Brain Mapp* 17:143–155
- Stinear CM, Barber PA, Smale PR, Coxon JP, Fleming MK, Byblow WD (2007) Functional potential in chronic stroke patients depends on corticospinal tract integrity. *Brain* 130:170–180
- Sukal TM, Ellis MD, Dewald JPA (2007) Shoulder abduction-induced reductions in reaching work area following hemiparetic stroke: neuroscientific implications. *Exp Brain Res* 183:215–223
- R Core Team (2016) R: a language and environment for statistical computing. R Foundation for Statistical Computing. <https://www.R-project.org/>. Accessed 1 Dec 2016
- Turton A, Wroe S, Trepte N, Fraser C, Lemon RN (1996) Contralateral and ipsilateral EMG responses to transcranial magnetic stimulation during recovery of arm and hand function after stroke. *Electroencephalogr Clin Neurophysiol* 101:316–328
- Veerbeek JM, Kwakkel G, van Wegen EEH, Ket JCF, Heymans MW (2011) Early prediction of outcome of activities of daily living after stroke: a systematic review. *Stroke* 42:1482–1488
- Veerbeek JM, van Wegen E, van Peppen R, van der Wees PJ, Hendriks E, Rietberg M, Kwakkel G (2014) What is the evidence for physical therapy poststroke? a systematic review and meta-analysis. *PLoS One* 9:e87987-33
- Ward NS, Newton JM, Swayne OBC, Lee L, Thompson AJ, Greenwood RJ, Rothwell JC, Frackowiak RSJ (2006) Motor system activation after subcortical stroke depends on corticospinal system integrity. *Brain* 129:809–819
- Welham S, Cullis B, Gogel B, Gilmour A, Thompson R (2004) Prediction in linear mixed models. *Aust NZ J Stat* 46:325–347
- Yao J, Dewald JPA (2018) The increase in overlap of cortical activity preceding static elbow/shoulder motor tasks is associated with limb synergies in severe stroke. *NRR* 32(6–7):624–634
- Zaaimi B, Edgley SA, Soteropoulos DS, Baker SN (2012) Changes in descending motor pathway connectivity after corticospinal tract lesion in macaque monkey. *Brain* 135(7):2277–2289

Publisher's Note Springer Nature remains neutral with regard to jurisdictional claims in published maps and institutional affiliations.